  Bull. Chem. Soc. Jpn., 56, 1289—1300 (1983)

Fluorescence Spectrum and Its Intensity of Europium Tris(ethyl sulfate) Enneahydrate

Tomoyuki Ohoka and Yoshifumi Kato*

Department of Chemistry, Faculty of Science, Kobe University Nada-ku, Kobe 657

(Received June 24, 1982)

The polarized fluorescence spectrum of the europium tris(ethyl sulfate) enneahydrate crystal was measured at 95 K by using excitation lines of an Ar^+ laser. The multipole character of transitions and the energies and crystal quantum numbers for the crystal field components of the $^7F_J(J=0, 1,\cdots,6)$ and $^5D_{0,1}$ terms were determined from the spectral analysis. It was ascertained that most of the transitions were due to forced electric dipole transitions but some of them due to magnetic dipole transitions, in which nine strong lines appeared as magnetic dipole radiations satisfying the selection rule for ion levels, while three weak lines were magnetic dipole radiations forbidden in ions. The relative intensities of both the forbidden electric dipole transitions and the magnetic dipole transitions were calculated by the crystal field wavefunctions obtained to reproduce the experimental data. From the comparison of the calculated intensities with the observed ones, the ratio of the populations of the $^5D_0$ term to the $^5D_1$ term in fluorescent process was estimated to be about 20, although the $^5D_0$ term was 1750 cm^{-1} lower than the $^5D_1$ term. The result suggested that the configuration mixing due to *g*-orbitals was significant to allow electric dipole transitions.

It has been already well known[1] that the trivalent europium ion of $4f^6$ configuration has a regular ^7F_J multiplet followed by a ^5D_J multiplet and is the only one with a nondegenerate ground state $^7F_0$ among trivalent rare earth metal ions. For the europium tris(ethyl sulfate) enneahydrate, $Eu(C_2H_5SO_4)_3\cdot 9H_2O$ (Eu(ES)), Sayre and Freed[2] determined most of the crystal field components of $^7F_J(J=0,1,\cdots,6)$ terms from the polarized fluorescence spectrum and partially analysed the ultraviolet absorption spectrum. They also pointed out that some of fluorescence lines with $\Delta J=\pm 1$ in the $^5D_{0,1}\rightarrow{}^7F_{0,1,2}$ transitions were due to magnetic dipole (MD) radiation and not due to electric dipole (ED) radiation from the polarization measurements, although the transition probability due to MD transitions is, in general, extremely smaller than that due to ED transitions for parity-allowed transitions (see Appendix A). Similar MD transitions were also observed in the fluorescence spectra of Eu^{3+} and Tb^{3+} in $LaCl_3$ by Dieke *et al.*,[3,4] where only MD transitions satisfying the selection rule for ions ($\Delta J=0, \pm 1$) were observed in the crystals. Hellwege *et al.*[5,6] separately determined the energies and quantum numbers of the crystal field components of the $^7F_{0,1}$, $^5D_{0,1,2}$, and several electronic terms in the ultraviolet region from the absorption spectrum of Eu(ES) and its Zeeman effect.

The present paper deals with a further investigation of the crystal field components of the ^7F_J terms in Eu(ES) from the polarization properties of the laser-excited fluorescence spectrum at the liquid nitrogen temperature. The laser-excited technique is anticipated to give detailed information for the energy levels of a crystal, because of powerful capacity of laser as a light source and the facility of selective excitation to a specific ion level in crystals. Then the fluorescence transition probabilities for both the forbidden ED transitions and the allowed MD transitions are calculated from the wavefunctions which have been determined to reproduce the observed crystal field levels by using the tensor-operator method.[7] Some discussions are presented by comparing calculated relative intensities with observed ones.

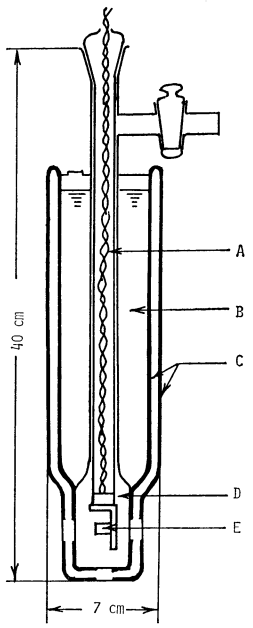

Fig. 1. Glass Dewar vessel for fluorescence measurements at liquid nitrogen temperature. A: Thermocouple, B: liquid nitrogen, C: silver plating, D: nitrogen gas, E: crystal.

Experimental

Preparation of the compound and the crystal growth were described in a previous paper.[8] A crystal was cut into a square rod of $3\times 3\times 8$ mm^3 with the largest side along the principal axis of the crystal. A single crystal was attached to a copper block in a special glass Dewar vessel (Fig. 1), which was filled with nitrogen gas at atomospheric pressure to prevent dehydration of crystalline water under vacuum. Since a crystal was cooled by heat conduction through nitrogen gas, the temperature of the crystal measured by a thermocouple was 95 K under incident Ar^+ laser beam at the liquid nitrogen temperature. The fluorescence spectrum was measured under a 90° scattering geometry by a Spex 14018 double spectrometer equipped with a cooled RCA C31034 photomultiplier and a Coherent Radiation model CR-4 Ar^+ laser. The exciting lines of 457.9 nm (21837

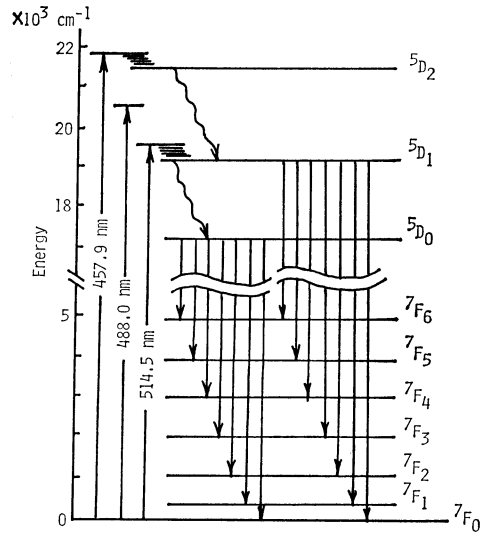

Fig. 2. Energy level diagram and observed fluorescence process of $Eu(C_2H_5SO_4)_3 \cdot 9H_2O$.

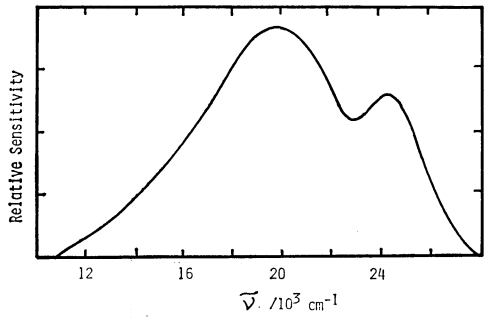

Fig. 3. Intensity response curve of the apparatus. The ordinate is in an arbitrary unit.

cm^{-1}) and 514.5 nm (19435 cm^{-1}) produced fairly intensive fluorescence and the fluorescence by the former was about 100 times as strong as that by the latter, while the exciting line of 488.0 nm (20492 cm^{-1}) scarcely produced fluorescence lines. This fact might easily be seen from the energy level diagram of the Eu^{3+} ion in Fig. 2. Almost all the electrons at 95 K occupy the lowest $^7F_0$ level and not the next $^7F_1$ level being about 380 cm^{-1} higher than the former. Thus, it is possible to produce directly the $^7F_0 \rightarrow {}^5D_2$ and $^7F_0 \rightarrow {}^5D_1$ excitations by the 457.9 and 514.5 nm exciting lines, respectively, and furthermore the former involves an ED transition allowed by the selection rule for crystal field levels, but the latter does not. Since such a condition is not satisfied by the 488.0 nm excitation, the 457.9 nm excitation yields the most intensive fluorescence. The measurement was carried out with the incident laser power of about 200 mW at the position of the crystal and the spectral slit-width was 4—10 cm^{-1} because most of fluorescence lines had intrinsically broad line-width even at 95 K. Wavenumbers were calibrated by already-known lines of neon, krypton, and argon discharge lamps. The accuracy of wavenumbers was within 1 cm^{-1}. The correction of the intensity response for the spectrometer-detector system as a function of wavenumber was performed by the calibration with a standardized tungsten source (Ushio No. 701038). The curve of the intensity response had the maximum at about 20000 cm^{-1} with gradual decrease toward low-wavenumber side and the relative intensity at 12000 cm^{-1} was about one-tenth of that at 20000 cm^{-1} (Fig. 3). The reproducibility of intensities

Table 1. Crystal quantum number classification for C_{3h} symmetry

J	M_J				No. levels
	$\mu=0$	$\mu=\pm1$	$\mu=\pm2$	$\mu=3$	
0	0				1
1	0	±1			2
2	0	±1	±2		3
3	0	±1	±2	$-3, +3$	5
4	0	±1	$\pm2, \mp4$	$-3, +3$	6
5	0	$\pm1, \mp5$	$\pm2, \mp4$	$-3, +3$	7
6	$-6, 0, +6$	$\pm1, \mp5$	$\pm2, \mp4$	$-3, +3$	9

Table 2. Selection rules for C_{3h} symmetry in case of even number of electrons

	For electric dipole					For magnetic dipole				
μ'	μ				μ'	μ			
	0	±1	±2	3		0	±1	±2	3
0			σ	π	0	σ	π		
±1		σ	π	σ	±1	π	σ	π	
±2	σ	π	σ		±2		π	σ	π
3	π	σ			3			π	σ

did not vary seriously over all the lines. The average accuracy of intensities was estimated to be within 15% except those for the very weak $^5D_{0,1} \rightarrow {}^7F_{5,6}$ transitions. However, the intensity of very weak transitions was considered to have a fairly large amount of error.

Fluorescence Spectra and Wavefunctions

According to the analysis of the crystal structure of rare earth metal tris(ethyl sulfate) enneahydrates,[9,10] the space group is $P6_3/m$ (C_{6h}^2) and the site symmetry around a rare earth metal ion is C_{3h}. A rare earth metal ion has nine water molecules as nearest neighbors, where the water oxygen atoms are at a distance of about 2.4 A from the metal ion. An ion level $|JM)$ under a crystal field splits into several crystal field levels which are designated by the crystal quantum number μ originally introduced by Hellwege[11] and thereafter partially extended by others.[1] The classification of levels split by C_{3h} symmetry of a given J term is tabulated in Table 1, where the level with double signs is twofold degenerate. The selection rules for ED and MD transitions in C_{3h} symmetry are shown for an even number of electrons in Table 2.[12] The fluorescence spectra of Eu(ES) excited by the 457.9 and 514.5 nm lines of an Ar^+ laser at 95 K are shown in the range from about 19000 to 14000 cm^{-1} in Figs. 4 and 5, where σ- (Fig. 4) and π-polarized (Fig. 5) spectra stand for the radiation emitted in directions perpendicular and parallel to the principal axis of a crystal, respectively. In these figures, all the lines except V, V(O–H), V(C–H), and Vib Raman are due to the fluorescence. The distinction between fluorescence lines and vibrational Raman lines could easily be made when the polarized spectra excited by the 457.9 and 514.5 nm lines are compared with

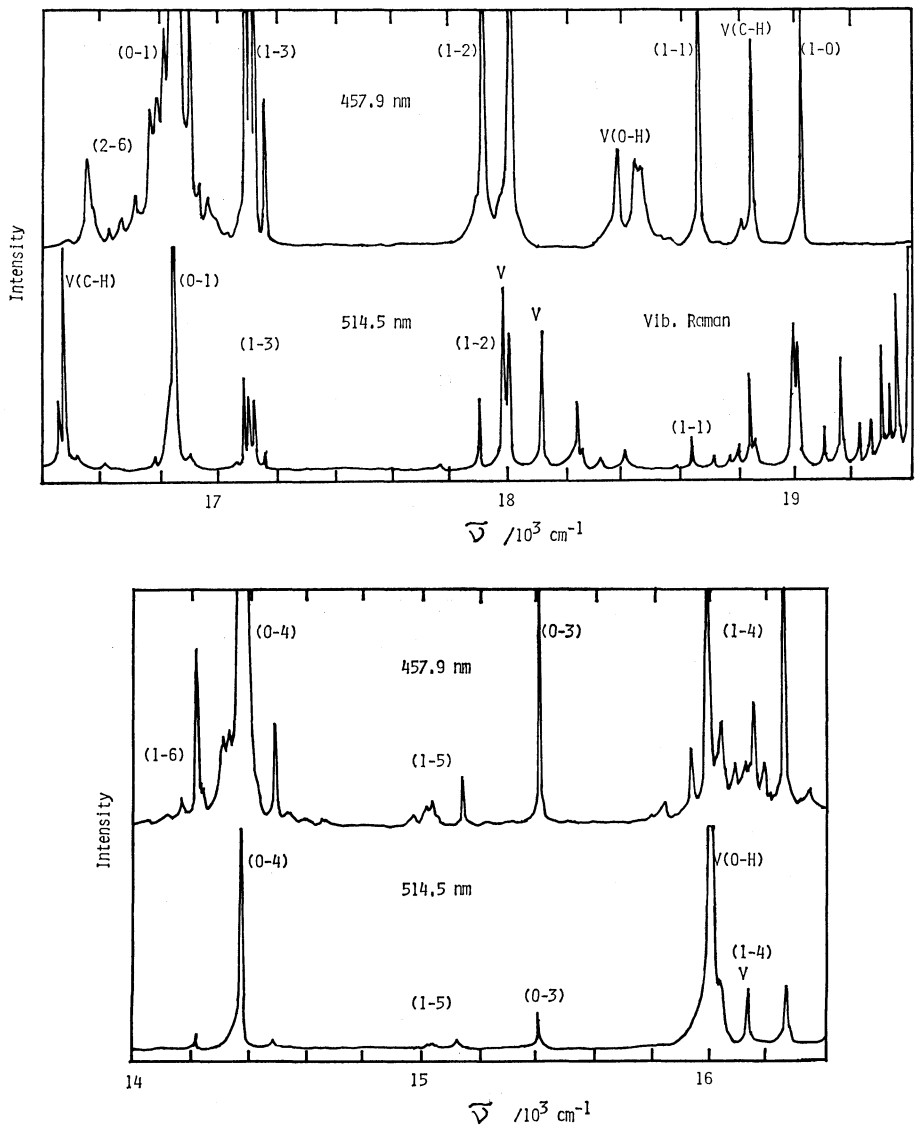

Fig. 4. σ-polarized fluorescence spectra of $Eu(C_2H_5SO_4)_3 \cdot 9H_2O$ at 95 K by the exciting lines of 457.9 nm (21837 cm^{-1}) and 514.5 nm (19435 cm^{-1}) of Ar^+ ion laser. Fluorescence lines between ^5D_J and $^7F_{J'}$ are shown by the notations of (J-J'). Notations of V, V(C–H),V(O–H), and Vib Raman indicate the vibrational Raman lines.

those by the 488.0 nm line or the polarized spectra of La(ES) without f electrons. In the latter spectra there were no fluorescence lines. Observed vibrational frequencies of polarized Raman spectra of Eu(ES) and La(ES) at 95 K are given in Table 3, where ZX- and ZZ-polarizations correspond to σ- and π-polarizations for fluorescences, and also to A_g and E_{1g} irreducible representations for vibrations, respectively. Although the fluorescence lines by the 457.9 nm excitation partially overlap with weak lines from the $^5D_2$ manifold, the latter lines could readily be distinguished from the $^5D_{0,1} \rightarrow {}^7F_J$ lines by comparing with the spectra of the 514.5 nm excitation. Thus the fluorescence lines were reasonably assigned to the transitions between crystal field levels. The nature of radiations was also clarified from the polarization properties following the selection rules and the result of calculated transition probabilities (see later section). The result obtained is given in Table 4, together with observed relative intensities. It can be seen in Table 4 that nine strong MD transitions are observed in the $^5D_{0,1} \rightarrow {}^7F_{0,1,2}$ transitions (the case of $\Delta J = \pm 1$ allowed for ions), and furthermore three very weak MD transitions are also observed in the $^5D_0 \rightarrow {}^7F_{3,4,5}$ transitions (the case of $|\Delta J| > 1$ forbidden for ion), where ΔJ is the difference of J between ion levels regarding a transition. The former MD transitions are those presented already by Sayre and Freed,[2] and the latter MD transitions in case of $|\Delta J| > 1$ have not yet been reported for any rare earth crystals so far as we know. Such transitions should be allowed to occur when there exist considerable interactions between crystal field components belonging to ion levels with different J (J-mixing), in addition to strong spin-orbit interactions (see Appendix A). Since the terms $^5D_{0,1}$ consist of only the crystal field levels with $\mu = 0$ and ± 1, the levels with $\mu = 0$ in the lower terms ^7F_J are able to be determined only by MD

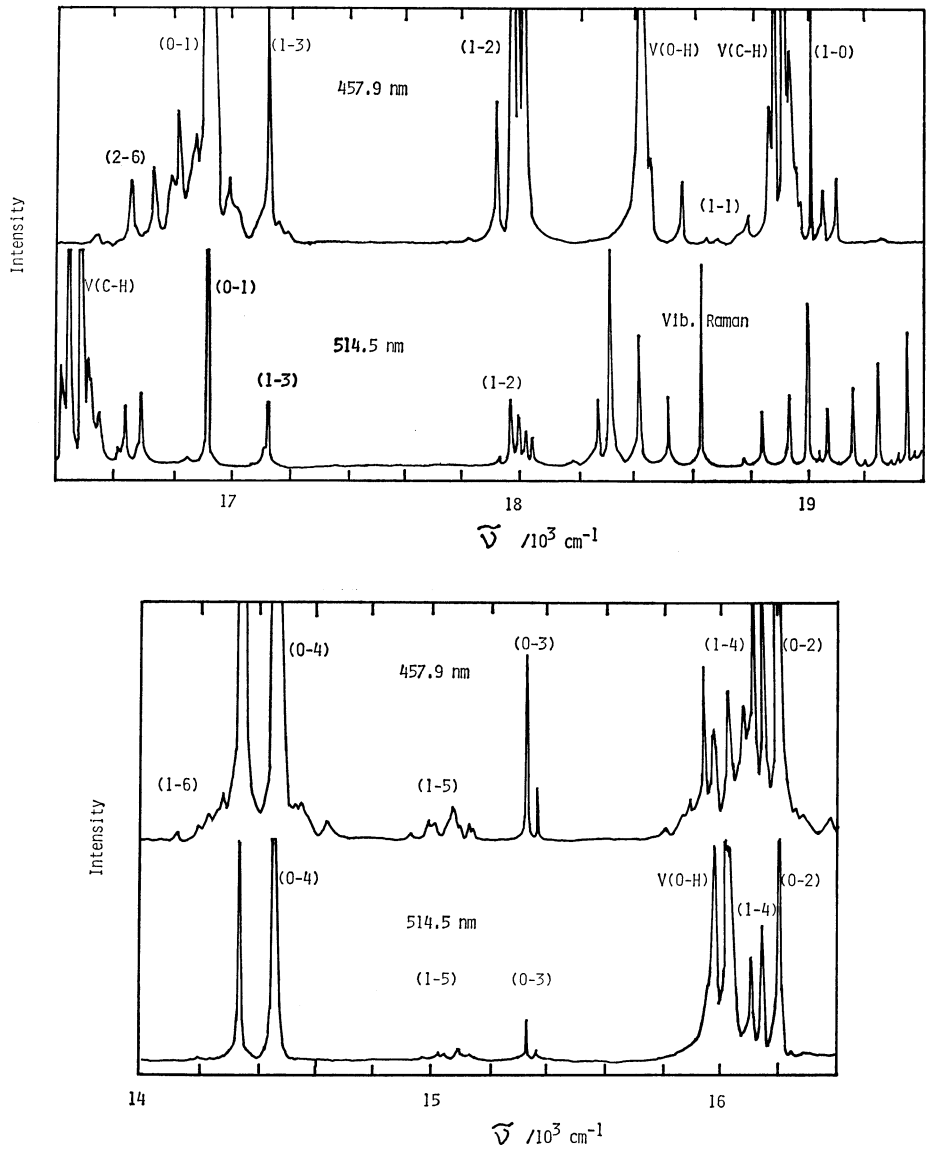

Fig. 5. π-polarized fluorescence spectra of $Eu(C_2H_5SO_4)_3 \cdot 9H_2O$ at 95 K by the exciting lines of 457.9 nm (21837 cm^{-1}) and 514.5 nm (19435 cm^{-1}) of Ar^+ ion laser. Notations are the same as in Fig. 4.

transitions and not by ED transitions as can be seen in the selection rules (Table 2). Observed energies and quantum numbers of crystal field levels are compared with those by Sayre and Freed[2] as given in Table 5. In both the results, there are few discrepancies between them regarding the wavenumbers and the crystal quantum numbers, but the $\mu=0$ levels in the $^7F_{3,4,5}$ terms are first acertained by the present analysis, and the present energy values are more accurate.

Wavefunctions. In order to calculate theoretically the transition probability between crystal field levels, it is necessary to have reliable wavefunctions in a crystal. Under intermediate coupling the wavefunctions of a rare earth metal ion are expressed by

$$|\phi_n) = \sum_n c_n |f^N:qSLJ), \quad (1)$$

where q is additional quantum numbers specifying a state except S, L, and J. When such an ion is placed in a crystal field, crystal field wavefunctions are given as

$$|\phi_a) = \sum_i a_i |f^N:qSLJM). \quad (2)$$

The Hamiltonian in crystals can be written as

$$H = H_{ion} + H_{cry}, \quad (3)$$

where H_{ion} and H_{cry} are the ion and crystal-field parts of interactions, respectively. The H_{ion} part consisting of the Coulomb and spin-orbit interactions can be expressed by a linear combination of the terms with the Slater radial integrals F_n (n=2,4,6) and the spin-orbit coupling constant ζ_{4f}. We further take account of scalar two-body electrostatic interactions arising from the second-order perturbation energies. These contribute to the H_{ion} as the terms with three configuration interaction (CI) parameters α, β, and γ.[14,15] Here we approximate that the site symmetry at a rare earth metal ion is D_{3h} instead of C_{3h} as adopt-

Table 3. Observed frequencies of polarized vibrational spectra of lanthanum and europium tris(ethyl sulfate) enneahydrate crystals at 95 K

A_g(ZZ) Raman shift ν/cm^{-1}		E_{1g}(ZX) Raman shift ν/cm^{-1}		Assignment[b]
La(ES)[a]	Eu(ES)[a]	La(ES)	Eu(ES)	
	40 vw	32 s	38 s	lattice mode
49 m	56 m			
63 m	72 s	60 vs	68 s	
88 m	99 m	82 m	93 m	
113 m	125 w	104 m	116 m	
		122 m	140 m	
160 s	177 s			
185 vw		190 w	197 w	
		236 s	246 vw	
258 s	265 m	252 m	259 s	
340 m	370 m	305 m	321 m	δ(CCO)
424 vs	424 vs	418 m	419 m	$\rho_r(SO_3)$
		430 s	432 s	
575 m	574 sh	538 w	540 w	$\delta(SO_3)$
	579 m	575 m	576 m	
619 w	625 w	610 w	662 w	
		628 w	655 w	
			704 vw	
809 vs	810 vs			$\rho_r(CH_2)$
934 m	933 m			ν(C-C)
1009 s	1011 s			ν(S-O)
1072 s	1073 vs			ν(C-O)
1110 m	1111 m	1155 vw	1155 vw	ν(S-O)
1215 w	1213 w	1200 m	1201 m	
		1291 m	1292 m	$\rho_w(CH_2)$
1367 w	1367 w			$\delta(CH_3)$
1392 w	1393 w			
1459 sh	1460 sh	1446 s	1447 s	$\delta(CH_2)$
1465 s	1466 m			
2727 m	2725 m			comb
	2778 m			
2788 sh	2790 vw			
2866 m	2868 m			ν(C-H)
2895 sh	2894 sh			
2921 s	2920 s			
2946 vs	2944 vs			
2978 vs	2977 vs	2984 s	2986 s	
2994 s	2993 s			
3031 w	3031 w	3006 w	3007 w	
3375 w	3373 m	3374 m	3375 m	ν(O-H)
3397 w	3395 w	3390 m	3389 m	
3442 vs	3440 vs	3445 m	3446 m	

a) vs: Very strong, s: strong, m: medium, w: weak, vw: very weak, sh: shoulder. b) ν: Stretching, δ: bending, ρ_r: rocking, ρ_w: wagging, comb: combination. The assignment is based on the analysis of the internal modes of $La(C_2H_5SO_4)_3 \cdot 9H_2O$ and $La(C_2H_5SO_4)_3 \cdot 9D_2O$ at room temperature in a previous work (see Ref. 13).

ed by most of authors. The adequacy of this assumption has already been discussed by Margolis.[16] In practice, the site symmetry is D_{3h} as far as nine oxygen atoms of the crystalline waters as nearest neighbors are concerned, and the contributions of six ES ions as next nearest neighbors to the crystal field is considered to be very small. Then the crystal field potential of D_{3h} may be expanded by the irreducible tensor $C_n^{(k)}$ [12] as

$$H_{cry}(D_{3h}) = B_0^2 C_0^{(2)} + B_0^4 C_0^{(4)} + B_0^6 C_6^{(6)} + B_6^6 [C_6^{(6)} + C_{-6}^{(6)}], \quad (4)$$

in which B_n^k is the crystal field parameter to be determined from experimental data. The matrix element of the Hamiltonian is reduced by the tensor-operator technique.[12,17] Since we are interested in the crystal field levels of the $^5D_{0,1}$ and ^7F_J terms only, a set of limited electronic terms interacting strongly with these terms is considered, *i.e.*, ^7F, $^5D1$, $^5D2$, $^5D3$, ^5L, $^5G1$, $^5G2$, $^5G3$, $^3P1$, $^3P3$, and $^3P6$ terms, where a final index of terms is an additional index following the table of Nielson-Koster,[18] which corresponds to q in Eq. 1. The procedure of the parameter determination is described in a previous paper.[17] At first, the diagonalization of the H_{ion} part with F_2, F_4, F_6, ζ_{4f}, α, β, and γ as adjustable parameters was performed by fitting calculated values to the centers of gravity of J-manifolds (*i.e.*, the "ion level" in crystals) derived from the experiments. Secondly the crystal field parameters were determined from the deviations of crystal field levels regarding individual "ion level". Finally a minor readjustment of all the parameters was made by the least-squares method by diagonalizing the entire Hamiltonian. Thus the eigenvectors for the "ion levels" (the c_n in Eq. 1) and the crystal field levels (the a_i in Eq. 2) have been determined separately. The final parameters are given in Table 6. The wavefunctions determined are considered to be fairly reliable from the root mean square (rms) deviations evaluated for both ion levels and crystal field levels (Table 6).

Fluorescence Intensity

Judd[19] and Ofelt[20] independently derived the theory for the line strength of induced electric dipole transitions observed between states of rare earth metal ions within the $4f^N$ configuration imbedded in crystalline solids and solutions. Here the basic theory for ED transitions being known as the Judd-Ofelt theory and then the theory for MD transitions are outlined. The fluorescence intensity I in erg per sec of spontaneous emission between ψ_a and ψ_b states is given as

$$I(\psi_a:\psi_b) = g(\psi_a)N(\psi_a)hc\sigma A(\psi_a:\psi_b), \quad (5)$$

where $g(\psi_a)$ and $N(\psi_a)$ are respectively the degeneracy and the number of ions in the initial state ψ_a, σ is the transition frequency in cm^{-1}, and $A(\psi_a:\psi_b)$ is the spontaneous transition probability. The transition probability due to dipole radiations can be written as

$$A(\psi_a:\psi_b) = 64\pi^4\sigma^3[\chi_e|(\psi_a|\boldsymbol{D}_e|\psi_b)|^2 + \chi_m|(\psi_a|\boldsymbol{D}_m|\psi_b)|^2]/[3h(2J+1)], \quad (6)$$

Table 4. Fluorescence spectrum of $Eu(C_2H_5SO_4)_3 \cdot 9H_2O$

Lower level	Upper level: $^5D_0(0)$[a] Wavenumber[b] $\tilde{\nu}$/cm^{-1}	Int.[c]	Energy[d]	$^5D_1(\pm1)$[a] Wavenumber $\tilde{\nu}$/cm^{-1}	Int.	Energy	$^5D_1(0)$[a] Wavenumber $\tilde{\nu}$/cm^{-1}	Int.	Energy	Average energy[d]
$^7F_0(0)$				19020.3π	1.28*	0.0	19024.5σ	1.00*	0.0	0.0
$^7F_1(\pm1)$	16902.2π	141.*	358.8	18661.8σ	2.19	358.4	(18663.7π	0.03*	360.7)[e]	358.6
(0)	16863.1σ	123.*	397.9	(18623.0π	0.02*	397.2)[e]				397.9
$^7F_2(\pm1)$				18003.8σ	13.4*	1016.2	18007.7π	6.83*	1016.5	1016.4
(±2)	16227.1σ	28.8	1033.7	17985.6π	13.3*	1034.4				1034.1
(0)				17913.3π	1.73*	1106.7	17917.7σ	7.40*	1106.5	1106.6
$^7F_3(3)$	15403.2π	2.13	1857.4	17162.8σ	0.87	1857.0	17165.9π	0.14	1858.1	1857.5
(0)	15380.6σ	0.41*	1880.0							1880.0
(±2)	15357.1σ	2.85	1903.5	17115.7π	10.1	1904.1	17120.7σ	6.36	1903.3	1903.6
(3′)				17106.6σ	2.85	1913.2	17110.5π	2.38	1913.5	1913.4
(±1)				17091.6σ	9.77	1928.2				1928.2
$^7F_4(\pm2)$	14476.8σ	161.	2783.6	16235.7π	10.0	2783.8	(16240.0σ	0.25	2783.7)[e]	2783.7
(±1)				16176.6σ	6.38	2842.9	16181.2	4.60	2842.8	2842.9
(3)	14370.9π	159.	2889.4	16130.2σ	f)	2889.3				2889.4
(0)	(14369.2σ	0.50*	2892.0)[e]							2892.0
($\pm2'$)	14367.1σ	130.	2893.2	16125.8π	0.82	2893.7	16130.2σ	f)	2893.5	2893.5
(3′)	14202.9π	3.70	3057.4	15962.5σ	1.94	3057.0	15966.2π	7.84	3057.5	3057.3
$^7F_5(\pm1)$				15161.6σ	0.26	3857.6				3857.6
(±2)	13383.3σ	0.32	3876.8	15142.1π	0.75	3877.1	15146.4σ	0.47	3877.0	3877.0
($\pm1'$)				15111.1σ	0.25	3908.1				3908.1
(3)	13228.3π	1.43	3931.7	15088.2σ	1.10	3931.0				3931.4
($\pm2'$)	13264.7σ	0.34	3995.3	15024.1π	0.67	3995.1	15028.2σ	0.90	3995.2	3995.2
(0)	13242.8σ	0.38*	4017.2	15002.0π	0.46	4017.2	15006.6σ	0.91	4016.8	4017.1
(3′)				14954.6σ	0.60	4064.6	14959.8π	0.77	4063.6	4064.1
$^7F_6(3)$	12322.7π	0.50	4937.1	14083.2σ	0.18	4935.7				4936.4
(±2)	12307.2σ	1.26	4952.5							4952.5
(3′)	12288.0π	1.18	4971.7	14046.0σ	0.16	4972.9	14050.1π	0.05	4973.0	4972.5
($\pm2'$)	12273.8σ	4.09	4985.9	14032.8π	0.32	4986.1	14036.9σ	0.08	4986.2	4986.1
(±1)				14025.2σ	0.24	4993.7				4993.7
($\pm1'$)				14001.8σ	0.11	5017.1				5017.1

a) The calculated energy of the $^5D_0(0)$ level is 17256.3 cm^{-1} in vacuum. The observed energies of the $^5D_1(\pm1)$ and $^5D_1(0)$ levels are 19015.0 and 19019.2 cm^{-1} in vacuum, respectively. The lines with asterisk are due to MD transition. b) Wavenumbers in cm^{-1} observed in air. c) Relative intensity in case that the intensity of the $^5D_1(0) \rightarrow {}^7F_0(0)$ transition is taken as 1.00. d) Energies in vacuum. Units in cm^{-1}. e) Values in parentheses are less reliable. f) The sum of the intensities of the $^5D_1(\pm1) \rightarrow {}^7F_4(3)$ and $^5D_1(0) \rightarrow {}^7F_4(\pm2')$ transitions is 5.21.

where $\boldsymbol{D}_e$ and $\boldsymbol{D}_m$ are ED and MD operators, respectively, while χ_e and χ_m are the correction factors of the medium related to the refractive index of the medium. When assumed that the surrounding medium around a rare earth metal ion is optically isotropic, the two correction factors might be taken to be equal approximately.[21] After eliminating the frequency dependence of σ^4 and making the correction of the intensity response for observed intensities, a relative intensity may be written as

$$I_r(\psi_a:\psi_b) = g(\psi_a)N(\psi_a)[|(\psi_a|\boldsymbol{D}_e|\psi_b)|^2 + |(\psi_a|\boldsymbol{D}_m|\psi_b)|^2]/(2J+1). \quad (7)$$

The matrix elements in Eq. 7 can be evaluated theoretically if the crystal-field wavefunctions are available.

Matrix Element of Electric Dipole Operator. ED operator $\boldsymbol{D}_e$ is given as

$$\boldsymbol{D}_e = -e\sum_i \boldsymbol{r}_i(\boldsymbol{C}^{(1)}_\rho)_i = -e\boldsymbol{D}'_e, \quad (8)$$

where $\boldsymbol{C}^{(1)}_\rho$ is the irreducible tensor of rank 1 and $\rho=0$ gives the z-component corresponding to π-polarized radiation, while $\rho=\pm1$ gives the $(x\pm iy)$-components corresponding to σ-polarized radiation. An ED transition between states within the $4f^N$ configuration is parity-forbidden. According to the Judd-Ofelt theory, we consider that the admixing of $nl^{N-1}n'l'$ configurations of opposite parity to nl^N configuration arises from the addition of a static crystal field with odd parity to the Hamiltonian. Then a perturbed state $\psi_{a'}$ and perturbing odd potential V_{odd} are shown by

$$|\psi_{a'}) = |\psi_a) - \sum_\eta [(nl^{N-1}n'l':\eta|V_{odd}|\psi_a)/\Delta E(\eta)] \times |nl^{N-1}n'l':\eta), \quad (9a)$$

$$\Delta E(\eta) = E(nl^{N-1}n'l':\eta) - E(\psi_a) \simeq \Delta E(n'l'), \quad (9b)$$

Table 5. Crystal field energy levels of $Eu(C_2H_5SO_4)_3 \cdot 9H_2O$

Term	Present		Sayre-Freed[a)]	
	Crystal Q.N.	Energy/cm^{-1}	Crystal Q.N.	Energy/cm^{-1}
$^7F_0$	0	0.0	0	0.0
$^7F_1$	±1	358.6	±1	356.
	0	397.9	0	398.
$^7F_2$	±1	1016.4	0	1015.
	±2	1034.1	±2	1031.
	0	1106.6	±1	1106.
$^7F_3$	3	1857.5	3	1856.
	0	1880.0		
	±2	1903.6	±2	1903.
	3′	1913.4	3′	1913.
	±1	1928.2	±1	1929.
$^7F_4$	±2	2783.7	±2	2782.
	±1	2842.9	±1	2841.
	3	2889.4	3	2890.
	0	2892.0		
	±2′	2893.5	±2′	2893.
	3′	3057.3	3′	3056.
$^7F_5$	±1	3857.6	±1	3858.
	±2	3877.0	±2	3880.
	±1′	3908.1		
	3	3931.4	3	3937.
			±1′	3955.
	±2′	3995.2	3′	3997.
	0	4017.1	±2	4021.
	3′	4064.1		
$^7F_6$			±1	4915.
	3	4936.4	3	4937.
	±2	4952.5	±2	4958.
	3′	4972.5	3′	4976.
	±2′	4986.1	±2	4992.
	±1	4993.7	±1′	4996.
	±1′	5017.1		
$^5D_0$	0	17256.3	0	17257.
$^5D_1$	±1	19015.0	±1	19015.
	0	19019.2	0	19020.

a) See Ref. 2.

and

$$V_{\text{odd}} = \sum_i \sum_{t,p} A_{tp} r_i^t (\mathbf{C}_p^{(t)})_i, \tag{10}$$

where $|nl^{N-1}n'l':\eta)$ is a mixing state and the unperturbed state $|\psi_a)$ is given in Eq. 2. From the perturbation theory, the final expression for the matrix element of $\boldsymbol{D}'_e$ is written in tensor-operator technique as

$$\begin{aligned}(\psi_{a'}|\boldsymbol{D}'_e|\psi_{b'}) = &\sum_{i,j}\sum_{\lambda}\sum_{t,p} a_i^* b_j (-1)^{2J+S+L'+\lambda-M+p+\rho} \\ &\times \delta(S,S')(2\lambda+1)[(2J+1)(2J'+1)]^{1/2} \\ &\times \begin{pmatrix} l & \lambda & t \\ \rho & -p-\rho & p \end{pmatrix}\begin{pmatrix} J & \lambda & J' \\ -M & p+\rho & M' \end{pmatrix} \\ &\times \begin{Bmatrix} J & J' & \lambda \\ L' & L & S \end{Bmatrix} T(t,\lambda)(qSL\|\boldsymbol{U}^{(\lambda)}\|q'SL'),\end{aligned} \tag{11}$$

Table 6. Parameters and root mean square deviations of $Eu(C_2H_5SO_4)_3 \cdot 9H_2O$

	For 10 ion levels		For 32 crystal levels	
Parameter/cm^{-1}	F_2	393.8	B_0^2	167.8
	F_4	54.29	B_0^4	−504.7
	F_6	5.947	B_0^6	−615.3
	ζ_{4f}	1277.5	B_6^6	524.5
	α	48.5		
	β	−690.5		
	γ	990.5		
rms deviation/cm^{-1}		71.3		6.0

$$\begin{aligned}T(t,\lambda) = &A_{tp}\sum_{l'}(-1)^{l+l'}2(2l+1)(2l'+1) \\ &\times \begin{pmatrix} l & 1 & l' \\ 0 & 0 & 0 \end{pmatrix}\begin{pmatrix} l & t & l' \\ 0 & 0 & 0 \end{pmatrix}\begin{Bmatrix} 1 & \lambda & t \\ l & l' & l \end{Bmatrix} \\ &\times (R_{nl}|r|R_{n'l'})(R_{n'l'}|r^t|R_{nl})/\Delta E(\eta).\end{aligned} \tag{12}$$

Under the site symmetry of D_{3h}, the odd potential can be written as[20)]

$$V_{\text{odd}}(D_{3h}) = \sum_i \sum_t A_{t3} r_i^t (\mathbf{C}_3^{(t)} - \mathbf{C}_{-3}^{(t)})_i. \tag{13}$$

From the triangular condition for the n-j symbols in Eqs. 11 and 12 in case of $l=3$, the following relations can be shown,

$$\lambda = 2,4,6, \quad t = \lambda \pm 1, \quad l' = 2,4. \tag{14}$$

Since the parameters $T(t,\lambda)$ contain perturbing crystal field parameters A_{tp}, and radial integrals and energies regarding mixing states $|nl^{N-1}n'l':\eta)$, it is difficult to estimate the $T(t,\lambda)$ theoretically without introducing several drastic assumptions. In order to study the oscillator strength of a group of lines corresponding to the transitions between the components of a pair of J-manifolds, Judd[19)] carried out an ingenious simplification for the basic expression by supposing the energy differences in Eq. 12 as being independent of mixing states and by making the sum over M, M', and ρ. Then the resultant expression with a single set of three adjustable parameters could be directly related to the oscillator strength derived from lanthanide solution spectra and it satisfactorily reproduced the experimental results. However, we have followed an alternate parametrization proposed by Axe,[21)] which is appropriate to describe the relative intensity of the transitions between crystal field levels by taking the $T(t,\lambda)$ themselves as adjustable parameters. Following the Judd-Axe treatment, a line strength between J-manifolds $S(\varphi_n J:\varphi_m J')$ defined in crystals is given as

$$\begin{aligned}S(\varphi_n J:\varphi_m J') = &\sum_t \sum_\lambda (2\lambda+1)T(t,\lambda)^2 \\ &\times |(\varphi_n J|\boldsymbol{U}^{(\lambda)}|\varphi_m J')|^2/(2t+1).\end{aligned} \tag{15}$$

The matrix elements of the unit tensor of rank λ can be calculated by the eigenvectors of the "ion levels" given in Eq. 1 as

$$\begin{aligned}(\varphi_n J|\boldsymbol{U}^{(\lambda)}|\varphi_m J') = &\sum_{n,m} c_n^* c_m \delta(S,S')(-1)^{S+L'+J-\lambda} \\ &\times [(2J+1)(2J'+1)]^{1/2}\begin{Bmatrix} J & J' & \lambda \\ L' & L & S \end{Bmatrix} \\ &\times (f^N:qSL\|\boldsymbol{U}^{(\lambda)}\|f^N:q'SL').\end{aligned} \tag{16}$$

Consequently, the parameters $T(t,\lambda)$ may be evaluated

Table 7. Observed and theoretical relative line strengths in $Eu(C_2H_5SO_4)_3 \cdot 9H_2O$

Lower level	Upper level					
	S_{obsd}		S_{theo}			
	$^5D_0$	$^5D_1$	$^5D_0$		$^5D_1$	
			ED	MD	ED	MD
$^7F_0$		3.56				0.0243
$^7F_1$	405.	4.48		0.0938	$0.00551T(3,2)^2$	0.000037
$^7F_2$	57.6	64.5	$0.00747T(3,2)^2$		$0.00174T(3,2)^2$	0.208
$^7F_3$	8.24	52.3			$0.00987T(3,2)^2 + 0.00826[T(3,4)^2+T(5,4)^2]$	
$^7F_4$	745.	55.4	$0.0106[T(3,4)^2+T(5,4)^2]$		$0.0121[T(3,4)^2+T(5,4)^2]$	
$^7F_5$	3.13	11.6			$0.00499[T(3,4)^2+T(5,4)^2] + 0.000396[T(5,6)^2+T(7,6)^2]$	
$^7F_6$	12.4	1.89	$0.00167[T(5,6)^2+T(7,6)^2]$		$0.00255[T(5,6)^2+T(7,6)^2]$	

by the line strengths derived from experiments and the calculated values of $(\varphi_n J|\boldsymbol{U}^{(\lambda)}|\varphi_m J')$. Now the number of $T(t,\lambda)$ to be evaluated is five from the restriction in Eq. 14; $T(3,2)$, $T(3,4)$, $T(5,4)$, $T(5,6)$, and $T(7,6)$.

Matrix Element of Magnetic Dipole Operator. MD operator $\boldsymbol{D}_m$ is given as

$$\boldsymbol{D}_m = -\beta(2\boldsymbol{S}+\boldsymbol{L}) = -\beta\boldsymbol{D}'_m, \quad \beta = -eh/(4\pi mc). \tag{17}$$

As MD operator is of even parity, MD transitions are allowed between states within the $4f^N$ configuration. The matrix element of MD transitions in crystals is reduced as

$$(\psi_a|(\boldsymbol{D}'_m)_\rho|\psi_b) = \sum_{i,j} a_i^* b_j (-1)^{J-M} \begin{pmatrix} J & 1 & J' \\ -M & \rho & M' \end{pmatrix} \times (f^N:qSLJ\|\boldsymbol{D}'_m\|f^N:q'S'L'J'), \tag{18}$$

where $\rho=0$ and ±1 correspond respectively to σ- and π-polarized radiations contrary to ED transitions. Following the results of Condon and Shortley,[22] the nonzero matrix elements must be diagonal in the quantum numbers q, S, and L, and furthermore the MD transitions are restricted by the selection rule on J ($\Delta J=0, \pm1$) to the following three cases:

1) $J'=J$,

$$(qSLJ\|\boldsymbol{D}'_m\|qSLJ') = g[J(J+1)(2J+1)]^{1/2}, \tag{19}$$

where

$$g = 1 + [J(J+1)+S(S+1)-L(L+1)]/[2J+1)].$$

2) $J'=J-1$,

$$(qSLJ\|\boldsymbol{D}'_m\|qSLJ') = \left[\frac{(S+L+J+1)(S+L+1-J)(J+S-L)(J+L-S)}{4J}\right]^{1/2}. \tag{20}$$

3) $J'=J+1$,

$$(qSLJ\|\boldsymbol{D}'_m\|qSLJ') = \left[\frac{(S+L+J+2)(S+J+1-L)(L+J+1-S)(S+L-J)}{4(J+1)}\right]^{1/2}. \tag{21}$$

After all, MD transition probability is able to be evaluated straightforwardly by using Eq. 1 for ion levels and Eq. 2 for crystal field levels, respectively.

Comparison of Observed and Calculated Intensities.

Populations of $^5D_{0,1}$ Terms: The observed relative line strengths S_{obsd} and theoretical ones S_{theo} from Eq. 15 for ED transitions and from the ion wavefunctions of Eq. 1 for MD transitions are tabulated in Table 7. Here, nonzero elements involving $T(t,\lambda)$ parameters for ED transitions are restricted by the triangular condition of the 6-j symbol in Eq. 16, whereas those for MD transitions are also limited by the selection rule of ion levels ($\Delta J=0, \pm1$). The S_{obsd} has been derived from the observed intensities by adding appropriate weights regarding the degeneracy of levels concerned and polarization measurements (see Appendix B). For the $^5D_0 \rightarrow {}^7F_{3,5}$ transitions, the S_{obsd} has been obtained from the experiments although these are very small, while there are no corresponding S_{theo} values for both ED and MD transitions. This fact solely results from the approximation adopted in the theory and may be explicable on the basis of the J-mixing effect of the crystal field interactions. The S_{obsd} values are still the quantity involving the populations of initial levels, while the S_{theo} values are independent of such population as be obvious from the definition. Thus, it is possible to estimate the population of initial levels. The fluorescent transitions originate from three crystal field levels; *i.e.*, the $^5D_0(0)$, $^5D_1(\pm1)$, and $^5D_1(0)$ levels. The $^5D_0(0)$ level is about 1750 cm^{-1} below the upper pair of nondegenerate $^5D_1(0)$ and doubly degenerate $^5D_1(\pm1)$ levels, and the two components of the $^5D_1$ term are separated by only 4.2 cm^{-1}. When we assume that three crystal field levels belonging to the $^5D_1$ term are populated identically by electrons, the ratio of the population of the $^5D_0$ to that of the $^5D_1$ is expressed as

$$\frac{N(^5D_0)}{N(^5D_1)} = \frac{S_{obsd}(^5D_0:{}^7F_J)/S_{theo}(^5D_0:{}^7F_J)}{S_{obsd}(^5D_1:{}^7F_{J'})/S_{theo}(^5D_1:{}^7F_{J'})} = R(^5D_0 \rightarrow {}^7F_J:{}^5D_1 \rightarrow {}^7F_{J'}), \tag{22}$$

here $N(^{2S+1}L_J)$ stands for the sum of populations over all the components of a J-manifold. Although the S_{obsd} of the $^5D_1 \rightarrow {}^7F_{1,2}$ transitions can arise from both ED and MD transitions, it will be supposed undoubtedly from the comparison of the order of magnitudes for the S_{obsd} and S_{theo} regarding the $^5D_1 \rightarrow {}^7F_{0,1,2}$ transitions that the $^5D_1 \rightarrow {}^7F_1$ transition is dominantly due to ED transition, while the $^5D_1 \rightarrow {}^7F_2$ transition is

Table 8. Ratios of parameters $T(t,\lambda)$

	$T(3,4)/T(3,2)$	$T(5,4)/T(3,2)$	$T(5,6)/T(3,2)$	$T(7,6)/T(3,2)$
Present	0.0130	3.01	−0.593	−0.712
Axe[a)]	0.000	−3.52	—	—

a) Data from Ref. 21.

Table 9. Comparison of observed and calculated relative transition probabilities

Lower level	Upper level: $^5D_0(0)$ Calcd ED	$^5D_0(0)$ Calcd MD	$^5D_0(0)$ Obsd	$^5D_1(\pm1)$ Calcd ED	$^5D_1(\pm1)$ Calcd MD	$^5D_1(\pm1)$ Obsd	$^5D_1(0)$ Calcd ED	$^5D_1(0)$ Calcd MD	$^5D_1(0)$ Obsd
$^7F_0(0)$					3.07	1.28		2.59	1.00
$^7F_1(\pm1)$		6.95	6.95	1.84	0.007	2.19		0.003	0.03
(0)		6.96	6.06		0.0	0.01			
$^7F_2(\pm1)$		0.004		0.50	12.0	13.4		5.91	6.83
(±2)	1.42		1.42	0.013	12.1	13.4	0.31		0.0
(0)					1.83	1.73		8.19	7.40
$^7F_3(3)$	0.044		0.10	0.68		0.87	0.0		0.14
(0)		0.015	0.02						
(±2)	0.061		0.14	9.82	0.002	10.1	3.01		6.38
(3′)				3.70		2.85	3.25		2.38
(±1)				7.96	0.045	9.77		0.033	0.0
$^7F_4(\pm2)$	5.55		7.93	9.31	0.0	10.1	0.49		0.25[a)]
(±1)		0.005	0.0	6.40	0.002	6.38	3.96	3.96	4.60
(3)	8.58		7.83	3.66		b)			
(0)		0.033	0.03						
$(\pm2')$	2.33		6.40	0.79	0.003	0.82	2.34		b)
(3′)	0.0		0.18	1.50		1.94	6.76		7.84
$^7F_5(\pm1)$				0.11	0.0	0.26			
(±2)	0.0082		0.02	1.21	0.0	0.75	0.39		0.47
(±1)				0.085	0.004	0.25			
(3)	0.075		0.07	0.78		1.10			
$(\pm2')$	0.023		0.02	1.71	0.014	0.67	1.46		0.90
(0)		0.016	0.02						
(3′)				0.73		0.60	1.68		0.77
$^7F_6(3)$	0.032		0.02	0.14		0.18			
(±2)	0.11		0.06	0.071	0.003	0.0			
(3′)	0.0		0.06	0.033		0.16	0.030		0.05
$(\pm2')$	0.031		0.20	0.016	0.0	0.32	0.085		0.08
(±1)		0.003	0.0	0.14	0.0	0.24			
$(\pm1')$				0.0	0.004	0.11		0.002	0.0

a) Less accurate value for the overlap due to the $^5D_0(0) \rightarrow {}^7F_2(\pm2)$ transition. b) The sum of the relative transition probabililities for the $^5D_1(\pm1) \rightarrow {}^7F_4(3)$ and $^5D_1(0) \rightarrow {}^7F_4(\pm2')$ transitions is 5.21.

mainly due to MD transition. Then, by substituting the values given in Table 7 into Eq. 22, the population ratios can be evaluated from several possible pairs of transitions as

$$R(^5D_0 \rightarrow {}^7F_1 : {}^5D_1 \rightarrow {}^7F_2) = 17.9 \quad \text{(MD character)} \qquad (23a)$$

$$R(^5D_0 \rightarrow {}^7F_2 : {}^5D_1 \rightarrow {}^7F_1) = 16.9 \quad \text{(ED character)} \qquad (23b)$$

$$R(^5D_0 \rightarrow {}^7F_4 : {}^5D_1 \rightarrow {}^7F_4) = 29.6 \quad \text{(ED character)} \qquad (23c)$$

$$R(^5D_0 \rightarrow {}^7F_6 : {}^5D_1 \rightarrow {}^7F_6) = 16.9 \quad \text{(ED character).} \qquad (23d)$$

The average value of the ratios becomes 20.3 and agrees well with Axe's estimate[21] (=19) which was estimated from only a set of MD transitions corresponding to Eq. 23a by similar analysis. Since the population ratio of the $^5D_0$ term to one crystal field component of the $^5D_1$ term is only seven, it will be seen that the electron population on upper levels in fluorescent process extremely deviates from the Boltzmann distribution as be expected. Strictly speaking, as the fluorescence intensity must be proportional to the population difference between two levels concerned and not to the population of only the upper level, the population ratio should be estimated from

the intensities of transitions terminating to the same level. Therefore, the fact that the ratios from both Eqs. 23a and 23b are nearly equal to those from Eqs. 23c and 23d may be interpreted as follows: The population of the $^7F_2$ term is almost equal to that of the $^7F_1$ term or small populations of these terms are neglected when compared with large populations on the upper terms $^5D_0$ and $^5D_1$. However, $R(^5D_0 \rightarrow {}^7F_1 : {}^5D_1 \rightarrow {}^7F_0)$ is 47.4 which is over twice as large as the ratio determined. This will probably result from the fact that there exists considerable intensity decrease due to self-absorption for the $^5D_1 \rightarrow {}^7F_0$ transition as will be seen later, or the electron population of the lowest ground $^7F_0(0)$ level is not always neglected when compared with the populations of the upper $^5D_0$ and $^5D_1$ terms.

Parameters $T(t,\lambda)$ and Relative Transition Probabilities: When both observed relative intensities I_r and line strengths S_{obsd} for all the transitions from only the $^5D_0$ term are divided by 20.3, resultant observed quantities are independent of the populations of initial levels and correspond to the relative transition probabilities obtained by experiments. Thus, the $T(t,\lambda)^2$ values can be evaluated by a least-squares method from the comparison of the S_{theo} and observed line strengths not involving the population for ED transitions. Furthermore, the determination of the sign of $T(t,\lambda)$ and a minor refinement are made to reproduce the experimental intensities between crystal field levels ascertained as ED transition. The final values of $T(t,\lambda)$ are given as the ratios to $T(3,2)$ in Table 8, together with Axe's estimate. The present values are in good agreement in magnitude with Axe's values, but the sign of $T(5,4)/T(3,2)$ differs from that of Axe. This fact will probably arise from the difference of both cases with respect to the method to reproduce the experimental results. In the present estimate, the final adjustment of the five $T(t,\lambda)$ values is performed for the $^5D_{0,1} \rightarrow {}^7F_J (J=0,1,\cdots 6)$ transitions by using the crystal field wavefunctions including complete J-mixing in Eq. 11, while Axe determined three parameters; $T(3,2)$, $T(3,4)$, and $T(5,4)$, for the $^5D_{0,1} \rightarrow {}^7F_J (J=0,1,\cdots 4)$ transitions to reproduce both the observed line strengths and the ratio of intensities between the Stark components only within individual J-manifolds by the wavefunctions without J-mixing determined from symmetry consideration alone. The comparison of observed transition probabilities between crystal field levels with calculated ones is given in Table 9, where the values are described as relative values by putting the calculated transition probability of the $^5D_0(0) \rightarrow {}^7F_1(\pm 1)$ for ED transitions and that of the $^5D_0(0) \rightarrow {}^7F_2(\pm 2)$ for MD transitions to be equal to the corresponding observed values, respectively. The agreement is considered to be satisfactory in view of the approximation used in calculations and the accuracy on experiments. Especially, the nature of radiations from the $^5D_1(\pm 1)$ level to degenerate levels $\mu=\pm 1$, and $\mu=\pm 2$ of the ^7F_J terms, which cannot be distinguished only from polarization measurements as be seen from the selection rules, is determined clearly from the calculated results. In Table 9, the calculated transition probabilities for

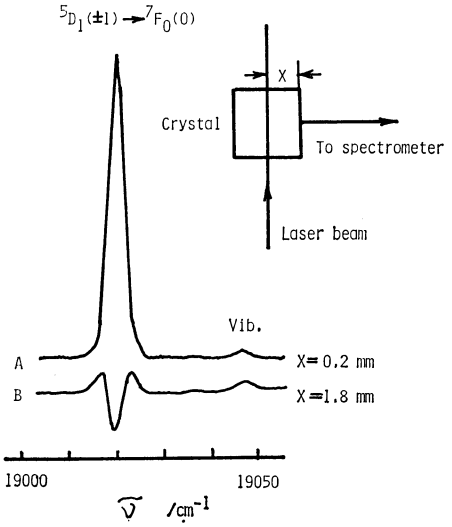

Fig. 6. π-polarized spectrum of the $^5D_1(\pm 1) \rightarrow {}^7F_0(0)$ transition of $Eu(C_2H_5SO_4)_3 \cdot 9H_2O$ at 95 K, showing self-absorption.

two MD transitions from the $^5D_1(0)$ and $^5D_1(\pm 1)$ levels to the lowest ground $^7F_0(0)$ level are considerably larger than the corresponding observed values. In practice, these MD transitions only showed heavily self-reserved line-shape in all the observed fluorescence lines when a laser beam passed through the middle of a crystal, as be seen in the case (B) of Fig. 6. Since self-absorption can occur when the absorbers and emitters are specially separated, we always attempted to pass an incident beam as close as possible to the crystal plane facing to a spectrometer (case (A) of Fig. 6). Such a fact that some of fluorescence lines to the lowest ground manifold only exhibit self-absorption at liquid nitrogen temperature has already been reported in other rare earth crystals.[23,24] Thus it does not seem to be an unjustifiable deduction to conclude that there still exists considerable intensity decrease for the above-mentioned MD transitions, although these line-shape did not show typical double humps even in a careful measurement. This phenomenon occurs in a 90° scattering measurement, but should be eliminated by 180° scattering.

Mixing Orbitals for Forbidden ED Transitions: Since the $T(t,\lambda)$ values are related to the radial wavefunctions $R_{n'l'}$ of mixing states, we introduce a parameter Γ following Axe[21] as

$$\Gamma = \sum_{n'} \Omega(n'g) / [\sum_{n'} \Omega(n'g) + \sum_{n'} \Omega(n'd)], \tag{24}$$

where

$$\Omega(n'l') = (R_{4f}|r|R_{n'l'})(R_{n'l'}|r^t|R_{4f})/\Delta E(n'l'). \tag{25}$$

Then the parameter Γ may be considered as a kind of measure on the contribution of admixing orbital $n'l'$ to allow ED transitions: $\Gamma=0$ means the contribution from d orbitals only, while $\Gamma=1$ is the contribution from g orbitals only. Appropriate ratios between $T(t,\lambda)$ values given in Eq. 12 are shown easily as a function of Γ as

$$\frac{T(3,4)}{T(3,2)} = \frac{1.95-1.42\Gamma}{1.0+1.50\Gamma}, \tag{26}$$

$$\frac{T(5,6)}{T(5,4)} = \frac{6.71-6.19\Gamma}{1.0+5.00\Gamma}. \quad (27)$$

Eq. 26 gives a maximum ratio of 1.95 for $\Gamma=0$ (pure d orbitals) and a minimum ratio of 0.212 for $\Gamma=1$ (pure g orbitals), whereas Eq. 27 gives a maximum ratio of 6.71 for $\Gamma=0$ and a minimum ratio of 0.081 for $\Gamma=1$. From the $T(t,\lambda)$ values of Table 8,

$$|T(3,4)/T(3,2)| = 0.0130, \quad |T(5,6)/T(5,4)| = 0.197. \quad (28)$$

Consequently, an unexpected conclusion that $n'g$ orbitals play a predominant role as configuration mixing for ED transitions is derived from both the cases. Dieke *et al.*[25] pointed out that the $4f^{N-1}5d$ configuration gave prominent contribution to emission spectra of the doubly and triply ionized rare earth metal ions. The present result, however, might not be somewhat surprising presumption when recognized that an $n'g$ orbital energy is not so higher than an $n'd$ orbital energy.

Appendix

(A) For an ED allowed transition in ions the oscillator strength f is of the order of magnitude one. An ED transition probability A^{E}_{ion} is related to the oscillator strength as[1]

$$A^{E}_{ion} = \frac{8\pi^2 e^2 \nu^2}{3mc^3} f = 2.68\times 10^9 (\sigma/Ry)^2 f, \quad (A1)$$

where σ is the wavenumber of transition and Ry is the Rydberg constant. Therefore, an ED allowed transition probability for a rare earth metal ion in crystals may be $10^8\ s^{-1}$ with a permissible factor of $10^{\pm 2}$ in the visible or near ultraviolet region. Since the ratio of an allowed MD transition probability, A^{M}_{ion}, to A^{E}_{ion} is expressed by $|[eh/4\pi mc]/e\langle r\rangle|^2$, A^{M}_{ion} becomes $10^2\ s^{-1}$. For the ED transition between the levels of the $4f^N$ configuration, the wavefunction must contain the terms of the configurations with odd parity. Thus the wavefunction is expanded by the perturbation theory as

$$\begin{aligned}|\psi_{a'}) = {} & |4f^N\psi_a : qSL) \\ & - \sum_k [(\varphi_k|H_{SO}|\psi_a)/\Delta E(4f)]\,|4f^N\varphi_k : qSLJ) \\ & - \sum_l [(\varphi_l|V_{even}|\psi_a)/\Delta E(4f)]\,|4f^N\varphi_l : qSLJM) \\ & - \sum_m [(\varphi_m|V_{odd}|\psi_a)/\Delta E(n'l')]\,|4f^{N-1}n'l'\varphi_m : qSLJM),\end{aligned} \quad (A2)$$

where the first term is unperturbed SL basis, and the second, third, and fourth terms are mixing states by the spin-orbit interaction, even- and odd-potential due to the crystal field, respectively. Here, $(\varphi_k|H_{SO}|\psi_a)$, $(\varphi_l|V_{even}|\psi_a)$, $(\varphi_m|V_{odd}|\psi_a)$, $\Delta E(4f)$, $\Delta E(n'l')$ may be the order of 10^2—10^3, 10^2, 10^2, 10^3—10^4, and 10^4—$10^5\ cm^{-1}$, respectively. Thus the transition probability responsible for crystal spectra is able to be expressed in terms of A^{E}_{ion} or A^{M}_{ion} as follows:

(I) for ED transition,

$$A^{E}_{cry} \simeq A^{E}_{ion}[(\varphi_k|H_{SO}|\psi_a)/\Delta E(4f)]^2 \times [(\varphi_m|V_{odd}|\psi_a)/\Delta E(n'l')]^2 = 10\ s^{-1}, \quad (A3)$$

(II) for MD transition ($\Delta J=0,\pm 1$),

$$A^{M}_{cry} \simeq A^{M}_{ion}[(\varphi_k|H_{SO}|\psi_a)/\Delta E(4f)]^2 = 1\ s^{-1}, \quad (A4)$$

(III) for MD transition ($|\Delta J|>1$),

$$A^{M}_{cry} \simeq A^{M}_{ion}[(\varphi_k|H_{SO}|\psi_a)/\Delta E(4f)]^2 \times [(\varphi_l|V_{even}|\psi_a)/\Delta E(4f)]^2 = 10^{-3}\ s^{-1}. \quad (A5)$$

Consequently, for the transitions within the $4f^N$ configuration the MD transition probability can be comparable to the ED forbidden one on some occasions. Especially, the $^5D_J \rightarrow {}^7F_{J'}$ transitions in a crystal are considered to be a further favorable case to yield MD transition, because these transitions also satisfy the selection rules for ion levels: $\Delta S=0,\pm 1$, $\Delta L=0,\pm 1$, and $\Delta J=0,\pm 1$. However, it will be easily found that even in the range of 20000 to 10000 cm^{-1} there are several fluorescence transitions of other triply ionized rare earth ions to satisfy the same conditions as the $^5D_J \rightarrow {}^7F_{J'}$ transitions of Eu^{3+} do; *e.g.*, $Nd^{3+}(^2H_{9/2}\rightarrow {}^4I_{9/2,11/2})$, $Sm^{3+}(^4G_{5/2}\rightarrow {}^6H_{5/2,7/2})$, $Tb^{3+}(^5D_4\rightarrow {}^7F_{3,4,5})$, $Er^{3+}(^2H_{11/2}\rightarrow {}^4I_{11/2,13/2})$, and $Tm^{3+}(^1G_4\rightarrow {}^3H_{4,5})$.

(B) The average intensity scattered from an ion or atom is associated with the intensities by polarization measurements,

$$I = \frac{1}{3}(I_X+I_Y+I_Z) \propto \frac{1}{3}(|\langle \boldsymbol{D}_X\rangle|^2+|\langle \boldsymbol{D}_Y\rangle|^2+|\langle \boldsymbol{D}_Z\rangle|^2), \quad (B1)$$

where I_X, I_Y, and I_Z are polarized intensities along X, Y, and Z axes in the space-fixed Cartesian coordinate, respectively, and $\langle \boldsymbol{D}\rangle$ is the matrix element of either the electric $\boldsymbol{D}_e$ or magnetic dipole moment $\boldsymbol{D}_m$. For an uniaxial crystal as rare earth tris(ethyl sulfate) enneahydrates, I_X must be equal to I_Y. One can estimate $I_X(|\langle(\boldsymbol{D}_e)_X\rangle|^2)$ and $I_Z(|\langle(\boldsymbol{D}_e)_Z\rangle|^2)$ from the intensities corresponding to σ- and π-polarized radiations for ED transitions respectively, whereas $I_X(|\langle(\boldsymbol{D}_m)_X\rangle|^2)$ and $I_Z(|\langle(\boldsymbol{D}_m)_Z\rangle|^2)$ or MD transitions are obtained inversely from π- and σ-polarization measurements. Consequently the average intensities are given as

$$\begin{aligned} I_e &= \frac{1}{3}(I_\pi+2I_\sigma) \quad \text{for ED transition,} \\ I_m &= \frac{1}{3}(I_\sigma+2I_\pi) \quad \text{for MD transition.}\end{aligned} \quad (B2)$$

This fact also may be verified analytically from direct estimate of the matrix elements of dipole moment operators in terms of $|JM)$ basis. In the evaluation of the line strength S_{obsd} (Table 7) from observed polarized intensities (Table 4), S_{obsd} is given as relative value by omitting the coefficient of 1/3 in Eq. B2.

This work was partially supported by a Grant-in-Aid for Scientific Research to Y. K. from the Ministry of Education, Science and Culture (No. 435045).

References

1) G. H. Dieke, "Spectra and Energy Levels of Rare Earth Ions in Crystals," Interscience Publ., New York (1968).
2) E. V. Sayre and S. Freed, *J. Chem. Phys.*, **24**, 1213 (1956).
3) L. G. DeShazer and G. H. Dieke, *J. Chem. Phys.*, **38**, 2190 (1963).
4) K. S. Thomas, S. Singh, and G. H. Dieke, *J. Chem. Phys.*, **38**, 2180 (1963).
5) K. H. Hellwege, U. Johnsen, H. G. Kahle, and G. Schaack, *Z. Phys.*, **148**, 112 (1957). The energies of the crystal field levels of the $^7F_1$ and $^5D_{0,1,2}$ terms given in this article are those at 294 K. Since the energy in crystals, in general, increases with the temperature rise, then the energies obtained at 95 K were several cm^{-1} less than those

by this article.
6) K. H. Hellwege, S. Hüfner, and A. Pöcker, *Z. Phys.*, **172**, 453 (1963).
7) G. Racah, *Phys. Rev.*, **62**, 438 (1942); **63**, 367 (1942); **76**, 1352 (1949).
8) Y. Kato, T. Nagai, and T. Nakaya, *Chem. Phys. Lett.*, **39**, 183 (1976).
9) D. R. Fitzwater and R. E. Rundle, *Z. Kristallogr.*, **112**, 362 (1959).
10) C. R. Hubbard, C. O. Quicksall, and R. A. Jacobson, *Acta Crystallogr., Sect. B*, **30**, 2613 (1974).
11) K. H. Hellwege, *Ann. Physik*, **4**, 95 (1949).
12) B. G. Wybourne, "Spectroscopic Properties of Rare Earths," Interscience Publ., New York (1965).
13) Y. Kato, T. Kurimoto, and T. Takenaka, *Spectrochim. Acta*, Part A, **33**, 1033 (1977).
14) K. Rajnak and B. G. Wybourne, *Phys. Rev.*, **132**, 280 (1963).
15) B. R. Judd, "Operator Techniques in Atomic Spectroscopy," McGraw-Hill, New York (1963).
16) J. S. Margolis, *J. Chem. Phys.*, **35**, 1367 (1967).
17) Y. Kato, T. Nagai, and A. Saika, *Bull. Chem. Soc. Jpn.*, **50**, 862 (1977).
18) C. W. Nielson and G. F. Koster, "Spectroscopic Coefficients for the p^n, d^n, and f^n Configurations," M. I. T. Press, Cambridge, Mass. (1963).
19) B. R. Judd, *Phys. Rev.*, **127**, 750 (1962).
20) G. S. Ofelt, *J. Chem. Phys.*, **37**, 511 (1962).
21) J. D. Axe, Jr., *J. Chem. Phys.*, **39**, 1154 (1963).
22) E. U. Condon and G. H. Shortley, "The Theory of Atomic Spectra," Cambridge Univ. Press, Cambridge, England (1957).
23) U. V. Kumar, D. R. Rao, and P. Venkateswarlu, *J. Chem. Phys.*, **67**, 3448 (1977).
24) Y. Kato, K. Okada, S. Hayashi, and T. Takenaka, *Chem. Phys. Lett.*, **61**, 266 (1979).
25) G. H. Dieke, H. M. Crosswhite, and B. Dunn, *J. Opt. Soc. Am.*, **51**, 820 (1961).